Supporting Information

to the paper

Electron stimulated hydroxylation of a metal supported silicate film

by Xin Yu, Emre Emmez, Qiushi Pan, Bing Yang, Sascha Pomp, William E. Kaden, Martin Sterrer, Shamil Shaikhutdinov, Hans-Joachim Freund, Itziar Goikoetxea, Radoslaw Wlodarczyk, Joachim Sauer

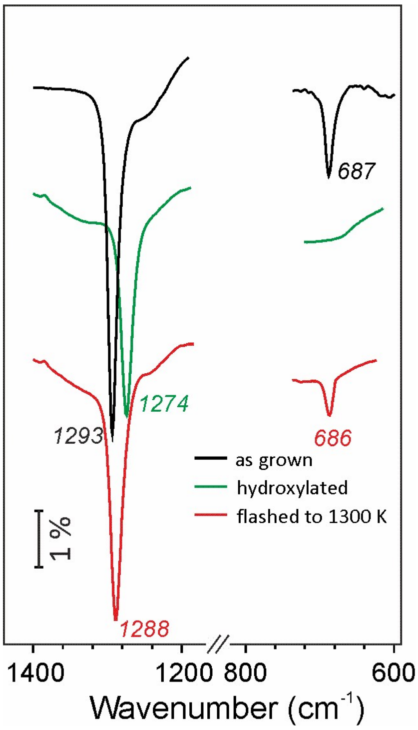

Figure S1. IRA spectra showing typical evolution of principal phonon bands upon treatment as indicated. The two bands of the “as grown” silicate film (i.e. at 1293 and 687 cm^{-1} in this case, black line) red-shift and attenuate after e-beam assisted hydroxylation (green line). The spectrum after subsequent flash to 1300 K in UHV is shown in red. It is clear that dehydroxylation does not fully recover the original structure of the film.

Scaling of OH and OD stretching wavenumbers

To compensate for systematic errors of DFT and neglected anharmonicities the calculated harmonic frequencies have been scaled by a factor f derived for the arithmetic mean of the symmetric (s) and antisymmetric (a) OH stretching frequencies as ratio of experimental (v), and calculated values (*ω)*

$f = ½ (\nu_s + \nu_a)/ ½ (\omega_s + \omega_a)$.

Table S1 shows both the scaling factors for $H^{16}O$, $D^{16}O$ and $D^{18}O$ bonds, together with the calculated and experimental results from which they are derived.

Table S1. Calculated harmonic frequencies (ω_i), experimental fundamental frequencies (v_i) (in cm^{-1}) and scaling factor f for $H_2{}^{16}O$, $D_2{}^{16}O$ and $D_2{}^{18}O$.

	calculated		experiment [a]		
	ω_a	ω_s	v_a	v_s	f
$H_2{}^{16}O$	3833.36	3720.19	3755.92	3657.05	0.9814
$D_2{}^{16}O$	2806.86	2679.53	2787.71	2671.64	0.9951
$D_2{}^{18}O$	2785.76	2668.60	2767.49	2660.79	0.9952

[a] Taken from Refs. [1, 2]

Calculated OH and OD stretching wavenumbers for structures Ia, Ib and II.

The oxygen atoms are labeled in the subscript according to Figure 7 in the main text. Oxygen isotope in the film and/or in surface hydroxyl is indicated in the superscript. The square of the dipole moment change in the direction normal to the surface ($<\mu_z>^2$) is shown in Debye^2/Å^2·amu.

Table S2. Calculated harmonic frequencies (cm^{-1}) for the hydroxylated silica bilayer structures on a Ru substrate without oxygen coverage.

	^{16}OH		^{16}OD//Si^{16}O$_2$		^{16}OD//Si^{18}O$_2$		^{18}OD//Si^{18}O$_2$	
	ν[a]	$<\mu_z>^2$	ν[b]	$<\mu_z>^2$	ν	$<\mu_z>^2$	ν[c]	$<\mu_z>^2$
Ia O_1D_1	3702	0.27	2733	0.41	2716[c]	0.38	2716	0.38
Ia O_2D_2	3617	0.31	2668	0.43	2668[b]	0.43	2652	0.41
Ib O_hD_h	3579	2.26	2640	3.19	2624[c]	3.01	2624	3.02
Ib O_tD_t	3757	2.22	2772	3.19	2772[b]	3.20	2755	3.00
II O_tD_t	3764	2.22	2778	3.18	2778[b]	3.18	2761	3.00

[a] Scaled (0.9814); [b] Scaled (0.9951); [c] Scaled (0.9952)

Table S3. Calculated harmonic frequencies (cm^{-1}) for the hydroxylated silica bilayer structures on a Ru substrate with a *p*(2 ×2)-O coverage.

	^{16}OH		^{16}OD//Si^{16}O$_2$		^{16}OD//Si^{18}O$_2$		^{18}OD//Si^{18}O$_2$	
	ν[a]	$<\mu_z>^2$	ν[b]	$<\mu_z>^2$	ν	$<\mu_z>^2$	ν[c]	$<\mu_z>^2$
Ia O_1D_1	3707	0.24	2736	0.36	2719[c]	0.34	2719	0.34
Ia O_2D_2	3637	0.32	2683	0.45	2683[b]	0.45	2667	0.43
Ib O_hD_h	3589	2.23	2647	3.15	2631[c]	2.98	2631	2.98
Ib O_tD_t	3737	2.11	2757	3.03	2757[b]	3.04	2741	2.84
II O_tD_t	3733	2.09	2755	2.98	2755[b]	2.99	2738	2.80

[a] Scaled (0.9814); [b] Scaled (0.9951); [c] Scaled (0.9952)

Effect of signal broadening for hydrogen-bonded O-D…O systems.

We follow Ugliengo and co-workers [3] who applied the empirical relation

$$\Gamma_i = 0.72\Delta_i + 2.5\ cm^{-1}$$

suggested by Huggins and Pimentel.[4] In the above equation Γ stands for the full width at half maximum, Δ is the frequency shift between the i^{th} frequency and the free OH frequency taken as reference. Although the proposed parameterization was designed for H, not for D, we use this in the first approximation for structure **Ib** on the Ru substrate without oxygen coverage. The O_tD_t vibration in this structure was used as the reference, and O_hD_h vibration as the one to correct. The frequency difference between these two bands is about 130 cm^{-1} which results in Γ = 96 cm^{-1}. The resulting spectrum is presented in Figure S2. Clearly, the O_hD_h related band is completely smeared out, and only the O_tD_t peak can be seen.

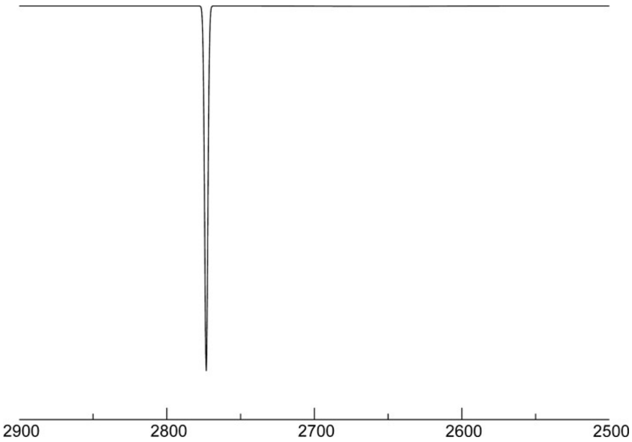

Figure S2. Simulated IRA spectrum in the OD region of structure Ib including the effect of signal broadening for O_hD_h group.

Calculated stretching wavenumbers of selected Si-O bonds in Ia, Ib and II.

The oxygen atoms are labelled in the subscript according to Figure 7 in the main text. Oxygen isotope in the film and/or in surface hydroxyl is indicated in the superscript. The square of the dipole moment change in the direction normal to the surface ($<\mu_z>^2$) is shown in Debye^2/Å^2·amu.

Table S4. Stretching wavenumbers (in cm^{-1}) of selected Si-O bonds in structure **Ia** on a Ru substrate with no oxygen coverage. Only vibrations with $<\mu_z>^2 > 3\ D^2$ are presented.

	^{16}OH		^{16}OD/Si^{16}O$_2$		^{16}OD/Si^{18}O$_2$		^{18}OD/Si^{18}O$_2$	
	ν	$<\mu_z>^2$	ν	$<\mu_z>^2$	ν	$<\mu_z>^2$	ν	$<\mu_z>^2$
Si-O-Si	1252	713	1252	712	1200	743	1200	742
	1172	3.1	1172	3.0	1118	2.8	1119	2.8
	1158	5.5	1157	6.0	1105	5.3	1105	5.3
SiO$_1$ stre	950	3.1	921	5.8	894	3.3	894	3.3
SiO$_2$ stre	860	8.1	854	5.0	850	3.3	832	4.5
Si-O-Si	678	18.2	669	44.9	657	21.0	656	20.9
	661	11.7	666	`6.8	646	2.9	644	0.7
	644	123	645	117	625	99.2	624	104
	620	81.6	618	36.3	594	96.0	594	92.2
	613	15.2	613	47.2	555	2.0	555	1.8

Table S5. Stretching wavenumbers (in cm^{-1}) of selected Si-O bonds in structure **Ib**, on a Ru substrate with no oxygen coverage. Only vibrations with $<\mu_z>^2 > 15\ D^2$ are presented.

	^{16}OH		^{16}OD/Si^{16}O$_2$		^{16}OD/Si^{18}O$_2$		^{18}OD/Si^{18}O$_2$	
	ν	$<\mu_z>^2$	ν	$<\mu_z>^2$	ν	$<\mu_z>^2$	ν	$<\mu_z>^2$
Si-O-Si	1244	665	1243	660	1191	695	1191	694
	1146	32.8	1145	27.0	1093	40.4	1093	40.5
	1136	13.5	1135	22.5	1082	13.6	1082	13.5
Si$_t$O$_t$ +Si$_a$O$_h$ anti-phase	940 *972*[a]	33.4	930	0.20	914 *945*[a]	31.0	901	0.40
Si$_t$O$_t$+Si$_a$O$_h$ in-phase	965 *998*[a]	31.1	906 *937*[a]	85.4	892 *923*[a]	47.4	880 *910*[a]	81.1
Si-O-Si	647	21.9	647	17.0	609	53.3	608	60.6
	631	56.9	644	5.3	596	117		
	616	120.7	625	153.4	594	11.7	595	119.6

[a] scaled (1.0341) [5]

Table S6. Stretching wavenumbers (in cm^{-1}) of selected Si-O bonds in structure **II** on a Ru substrate with no oxygen coverage. Only vibrations with $\langle\mu_z\rangle^2$ > 15 D^2 are shown.

	^{16}OH		^{16}OD/Si^{16}O$_2$		^{16}OD/Si^{18}O$_2$		^{18}OD/Si^{18}O$_2$	
	ν	$\langle\mu_z\rangle^2$	ν	$\langle\mu_z\rangle^2$	ν	$\langle\mu_z\rangle^2$	ν	$\langle\mu_z\rangle^2$
Si-O-Si	1251	733	1251	733	1199	768	1199	768
	1140	37.4	1140	37.7	1087	26.9	1087	26.8
Si$_t$O$_t$ + (Si$_a$O$_3$Ru)$_{as}$ in-phase	940	41.7	919	47.5	917	48.5	892	46.1
			950[a]		*948*[a]		*923*[a]	
(Si$_a$O$_3$Ru)$_{as}$+ Si$_t$O$_t$ antiphase	902	60.1	902	69.4	868	59.8	868	65.6
	933[a]		*933*[a]		*898*[a]		*898*[a]	
Si-O-Si	655	48.6	656	45.5	642	19.2	642	20.7
	618	144	619	147.3	597	91.4	596	145.0
(Si$_a$O$_3$Ru)$_s$ + (Si-O-Si)	528	16.2	528	15.5	515	18.4	515	18.9

[a] scaled (1.0341) [5]

Table S7. Stretching wavenumbers (in cm^{-1}) of selected Si-O bonds in structure **Ia** on a Ru substrate with a *p*(2 ×2)-O coverage. Only vibrations with $\langle\mu_z\rangle^2$ > 3 D^2 are presented.

	^{16}OH		^{16}OD/Si^{16}O$_2$		^{16}OD/Si^{18}O$_2$		^{18}OD/Si^{18}O$_2$	
	ν	$\langle\mu_z\rangle^2$	ν	$\langle\mu_z\rangle^2$	ν	$\langle\mu_z\rangle^2$	ν	$\langle\mu_z\rangle^2$
Si-O-Si	1253	728	1253	727	1200	758	1200	758
	1176	3.5	1176	3.5	1122	3.2	1122	3.2
	1158	6.9	1157	7.3	1105	6.6	1104	6.6
Si-O$_1$	948	2.7	919	5.3	892	3.2	891	3.1
Si-O$_2$	858	7.1	854	4.6	849	3.1	832	4.1
Si-O-Si	682	14.9	683	6.9	660	20.3	659	12.1
	666	8.9	669	30.8	657	2.6	656	10.8
	648	128	648	119	628	100	627	102
	623	99.5	622	47.0	608	12.3	608	13.1
	617	3.2	617	35.1	598	95.5	597	93.0
	605	1.6	614	6.0	558	2.3	557	2.1

Table S8. Stretching wavenumbers (in cm^{-1}) of selected Si-O bonds in structure **Ib,** on a Ru substrate with a *p*(2 ×2)-O coverage. Only vibrations with $<\mu_z>^2$ > 15 D^2 are presented.

	^{16}OH		^{16}OD/Si^{16}O$_2$		^{16}OD/Si^{18}O$_2$		^{18}OD/Si^{18}O$_2$	
	ν	$<\mu_z>^2$	ν	$<\mu_z>^2$	ν	$<\mu_z>^2$	ν	$<\mu_z>^2$
Si-O-Si	1244	670	1243	666	1191	701	1191	700
	1146	28.5	1145	23.2	1093	33.8	1093	33.9
	1134	12.8	1133	19.7	1080	13.0	1080	12.9
	1096	10.3	1096	14.7	1043	16.4	1043	16.4
Si_tO_t +Si_aO_h anti-phase	936	33.1	932	0.55	910	13.8	904	0.44
	968[a]				*941*[a]			
Si_tO_t+Si_aO_h in-phase	969	20.2	901	85.3	893	65.7	875	81.4
	1002[a]		*931*[a]		*923*[a]		*905*[a]	
Si-O-Si	645	18.1	648	17.0	635	5.4	634	5.0
	635	66.2	629	159	612	50.3	611	61.4
	620	122	616	37.7	599	123	598	125

[a] scaled (1.0341) [5]

Table S9. Stretching wavenumbers (in cm^{-1}) of selected Si-O bonds in structure **II**, on a Ru substrate with a *p*(2 ×2)-O coverage. Only vibrations with $<\mu_z>^2$ > 15 D^2 are shown.

	^{16}OH		^{16}OD/Si^{16}O$_2$		^{16}OD/Si^{18}O$_2$		^{18}OD/Si^{18}O$_2$	
	ν	$<\mu_z>^2$	ν	$<\mu_z>^2$	ν	$<\mu_z>^2$	ν	$<\mu_z>^2$
Si-O-Si	1252	737	1252	737	1199	774	1199	773
	1152	23.2	1152	23.1	1099	27.3	1099	27.4
	1139	46.3	1139	46.5	1085	34.3	1085	34.2
$(Si_aO_3Ru)_{as}$	978	141	978	141	938	128	938	131
			1012		*970*[a]		*970*[a]	
Si_tO_t	928	44.1	903	65.2	901	63.7	877	63.5
	960[a]		*934*[a]		*932*[a]		*907*[a]	
Si-O-Si	656	34.4	657	31.3	645	13.0	644	15.5
	640	10.9	639	9.9	605	13.4	602	30.0
	620	140	621	143	597	129	597	112
$(Si_aO_3Ru)_s$ + (Si-O-Si)	540	12.7	539	11.8	527	14.7	527	15.0

[a] scaled (1.0341) [5]

Calculations on an edingtonite-derived model for terminal silanol groups

As computational reference for isolated silanol groups on the external all-Si-zeolite surface we use a periodic edingtonite surface model as suggested by Ugliengo and co-workers (Civalleri et al., *J. Phys. Chem. B*, 1999, **103**, 2165-2171), see Döbler, Pritzsche, and Sauer, *J. Phys. Chem. C*, 113 (2009) 12454. It has a relatively small unit cell with a distance of 659 pm between the silanol groups at the hydroxylated (100) surface. The main structural feature of the zeolite is a cage consisting of three fused four-membered ring as shown in Fig. S3 below:

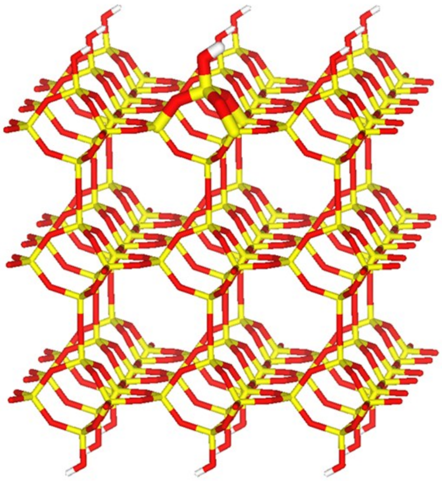

Figure S3. Periodic model of the fully hydroxylated edingtonite (100) surface.

For edingtonite, a (3 × 3) supercell has been used with a = 1976.04, b = 2120.46, c =5000 pm, $\alpha = \beta = \gamma$ =90º. The structure, shown in Fig. S3, was optimized by relaxing all the atomic positions. Due to the large amount of atoms involved in both structures, a partial Hessian approach was used to yield the vibrational frequencies of isolated silanols. The partial Hessian was restricted to a $(SiO)_3SiOH$ cluster (shown in bold sticks in Fig. S3).

With the scale factors of Table S1, we obtain the following wavenumbers for the terminal silanols of edingtonite: 3749 cm^{-1} for ^{16}OH, 2767 cm^{-1} for ^{16}OD and 2750 cm^{-1}for ^{18}OD.

References:

1. J. Tennyson, P. F. Bernath, L. R. Brown, A. Campargue, A. G. Csaszar, L. Daumont, R. R. Gamache, J. T. Hodges, O. V. Naumenko, O. L. Polyansky, L. S. Rothman, A. C. Vandaele, N. F. Zobov, A. R. Al Derzi, C. Fabri, A. Z. Fazliev, T. Furtenbacher, I. E. Gordon, L. Lodi and I. I. Mizus, *J Quant. Spectrosc. Radiat. Trans.*, 2013, **117**, 29-58.
2. J. Tennyson, P. F. Bernath, L. R. Brown, A. Campargue, A. G. Csaszar, L. Daumont, R. R. Gamache, J. T. Hodges, O. V. Naumenko, O. L. Polyansky, L. S. Rothman, A. C. Vandaele, N. F. Zobov, N. Denes, A. Z. Fazliev, T. Furtenbacher, I. E. Gordon, S. M. Hu, T. Szidarovszky and I. A. Vasilenko, *J Quant. Spectrosc. Radiat. Trans.*, 2014, **142**, 93-108.
3. F. Musso, M. Sodupe, M. Corno and P. Ugliengo, *J. Phys. Chem. C*, 2009, **113**, 17876-17884.
4. C. M. Huggins and G. C. Pimentel, *J. Phys. Chem.*, 1956, **60**, 1615-1619.
5. D. Löffler, J. J. Uhlrich, M. Baron, B. Yang, X. Yu, L. Lichtenstein, L. Heinke, C. Büchner, M. Heyde, S. Shaikhutdinov, H.-J. Freund, R. Wlodarczyk, M. Sierka and J. Sauer, *Phys. Rev. Lett.*, 2010, **105**, 146104.